55. W. G. Melson, S. R. Hart, G. Thompson, *Geol. Soc. Am. Mem.* **132**, 241 (1972).
56. M. K. Roden, S. R. Hart, G. Thompson, *Contrib. Mineral. Petrol.* **85**, 376 (1984).
57. E. Bonatti, *Nature* **345**, 800 (1990).
58. T. Staudacher *et al.*, *Earth Planet. Sci. Lett.* **96**, 119 (1989).
59. M. J. O'Hara, *Nature* **253**, 708 (1975); F. R. Boyd and R. B. McCalister, *Geophys. Res. Lett.* **3**, 509 (1976).
60. H. B. Dick and T. Bullen, *Contrib. Mineral. Petrol.* **86**, 54 (1984).
61. T. Shibata and G. Thompson, *ibid.* **93**, 144 (1986).

62. I am grateful to G. Ottonello, F. Sciuto, and R. Saxena for help in the geothermometry section, and to D. Walker and two anonymous reviewers for constructive comments. I thank D. Breger, P. Catanzaro, and K. Streech for help in putting together the manuscript. Research supported by the National Science Foundation. Lamont-Doherty Geological Observatory of Columbia University Contribution no. 4665.

14 May 1990; accepted 17 July 1990

Hematite Nanospheres of Possible Colloidal Origin from a Precambrian Banded Iron Formation

JUNG HO AHN* AND PETER R. BUSECK

Exceptionally small spheres (nanospheres) of hematite (diameters between 120 and 200 nanometers) occur in the Marra Mamba Iron Formation of the Hamersley Basin, Australia. The nanospheres are clustered into small aggregates and may have formed by structural ordering and dehydration of colloidal iron hydroxide particles. Individual spheres consist of numerous thin, curved hematite platelets surrounding a central void that is approximately half the diamter of the sphere; this texture suggests that they formed by a volume reduction of the original colloidal particles by ~12.5%. The occurrence of hematite nanospheres supports the hypothesis that some of the iron was deposited colloidally during the development of banded iron formations, approximately 2.5 billion years ago.

THE ORIGIN OF PRECAMBRIAN IRON formations, the world's oldest and largest iron deposits, has been a source of continuing interest and occasional controversy for many decades (*1–6*). They occur as layered rocks on all continents and provide the bulk of mined iron. Potentially, they indicate the character and history of the early Earth's oceans, atmosphere, and biosphere (*5–9*); they have been used to infer the evolution of Earth's atmosphere in Precambrian time. The methods of concentrating, transporting, and then depositing the vast quantities of iron in these extensive sedimentary units provide serious geological and geochemical problems.

Colloidal transport and deposition has been proposed as one means of moving the extraordinary amounts of iron to the basins where the iron ultimately was deposited (*10, 11*), but direct observational evidence has been both sparse and equivocal. Spherical structures 5 to 40 μm in diameter are common in iron formations, but there is dispute over whether they indicate purely chemical colloidal processes (*12–15*), organic activity (*16*), or recrystallization (*17*). In this paper we describe tiny hematite spheres that have diameters only 1/40 to 1/200 of known spherical features in iron formations. We propose these spheres as strong indicators of colloidal proceses during deposition of the iron formations.

We studied two samples that were selected to be representative of regions of drill core separated vertically by ~2 m. The core (D.D.H. No. 270, located 38 km west of Wittenoom, Australia) is from the Marra Mamba Iron Formation, which is of the Lake Superior type (*17a*). This formation was deposited about 2.5 billion years ago, at the approximate boundary between the Archean and Proterozoic ages and is the lowermost member of the Hamersley Group of Western Australia (*18*). In addition to the hematite, the samples contain quartz, magnetite, stilpnomelane, ankerite, minnesotaite or talc, and fibrous riebeckite (crocidolite). Specimens were examined at 400 and 120 kV with JEOL JEM-4000EX and Philips 400T transmission electron microscopes (*19*).

In all the grains that we observed, the hematite occurs in tiny clusters between quartz grains. Most hematite aggregates are smaller than 2 μm in diameter, and they have relatively sharp boundaries with the quartz (Fig. 1). Electron-diffraction patterns show rings as a result of the polycrystalline character of the aggregates (Fig. 2 and Table 1). These aggregates consist of spheres that have diameters between 120 and 200 nm (Fig. 3); we call them "nanospheres." The hematite nanosphere clusters are widespread in the specimens we studied. Only circular shapes were observed in our transmission electron microscopy (TEM) images, indicating that the hematite has a spherical rather than cylindrical form.

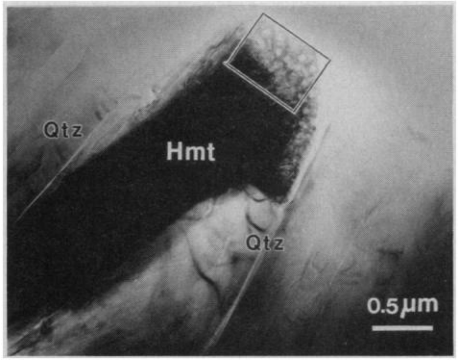

Fig. 1. Low-magnification TEM image showing a hematite cluster (Hmt) in quartz (Qtz).

The TEM images of the nanospheres show marked contrast between the outer shells and central areas (Fig. 3). These cores show light contrast and produce neither electron-diffraction patterns nor lattice fringes in TEM observations; only the outer shells consist of hematite. These shells consist of thin, subparallel, platy crystals, each approximately 3 to 5 nm thick (Fig. 4). Completely circular single crystals were not observed; instead, many curved crystals are joined to form spherical structures.

The appearance of the hematite nanospheres is similar to that of Fe-Si-Al-oxyhydroxides that crystallized from gel spheres (*20*). The presence of central voids suggests that the nanospheres also formed by void nucleation (*21*) from colloidal gels rather than by nucleation crystallization or spinodal decomposition. The central voids apparently formed during shrinkage caused by both ordering and dehydration.

Fine-grained hematite in weakly meta-

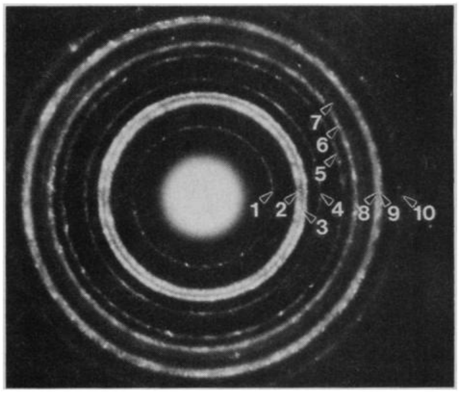

Fig. 2. Electron-diffraction pattern of hematite showing ring features. The ten innermost reflection rings are numbered; their interplanar spacings and indices are given in Table 1.

J. H. Ahn, Department of Geology, Arizona State University, Tempe, Arizona, 85287-1404.
P. R. Buseck, Departments of Geology and Chemistry, Arizona State University, Tempe, Arizona 85287-1404.

*Present address: Korea Ocean Research and Development Institute, Ansan P.O. Box 29, Seoul, Korea.

Fig. 3. TEM image of hematite showing spherical structures. This image corresponds to the area marked by a square in Fig. 1.

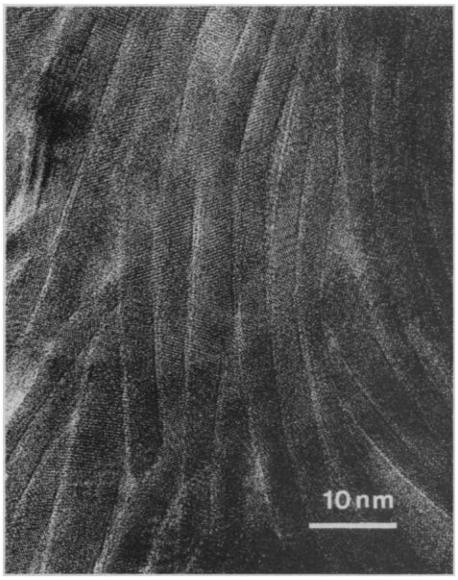

Fig. 4. High-resolution TEM image of thin platy hematite crystals forming a sphere. Various lattice fringes are shown in individual crystals. Most crystals are highly elongated and bent.

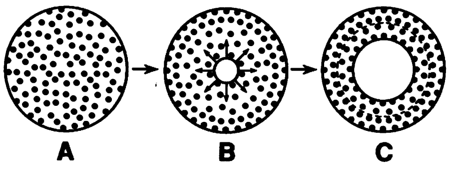

Fig. 5. Schematic diagram of the formation process of a hematite nanosphere from a colloidal particle, following the hypothesis of void nucleation (*20*). (A) Original iron hydroxide sphere consisting of a three-dimensional network of poorly ordered $Fe(OH)_3$. (B) Contraction results from partial ordering a dehydration of iron hydroxide; a void starts to form at the center of the sphere. (C) Complete dehydration and crystallization of hematite result in a significant decrease in volume.

morphosed iron formations is widely considered to be primary (*1, 12, 14, 22*). Such hematite retained its structural character unless it reacted to magnetite during higher grade metamorphism (*23*). The hematite in the nanospheres shows no textural evidence of being recrystallized and thus a secondary mineral, and so we believe it is a fine-grained primary hematite.

Colloidal particles of iron hydroxide have gel structures in which $Fe(OH)_3$ molecules form three-dimensional networks, and such particles easily crystallize to hematite (*24*). Spherical hematites having diameters of 100 and 190 nm have been synthesized (*25*). Hematite formation by structural rearrangement of iron hydroxide results in a volume decrease. In our samples contraction evidently formed central voids. We assume that the volume of the voids equals the volume difference between the original colloidal spheres and the resulting crystalline phases (Fig. 5). Such a sphere-forming process assumes that each nanosphere crystallized from an individual colloidal particle.

The final void size varies depending on the degree of structural ordering and on the water contents of the original colloidal particles. The diameters of most voids are about half those of the nanospheres; thus the hematite now occupies a volume that is ~12.5% less than the original colloidal particles. We hypothesize that crystallization of hematite started at the peripheries of the percursor particles and therefore that their original sizes were preserved. The sphere peripheries solidified upon hematite crystallization; the hard crusts presumably prevented inward shrinkage of collapse of the spherical shells, which still appear intact. The central voids suggest that during crystallization the nanospheres predominatly contracted from their interiors rather than from their exteriors (Fig. 5). Such shrinkage can be explained by strain differences at the outer and inner parts of the spherical shells and the influence of sphere diameter on crystallization rate. Large curvature in crystals produces more strain than small curvature, and crystals can grow faster in regions with less strain (*26*). Thus, hematite could form more rapidly along the exteriors of the precursor colloidal particles than along their interiors.

The uniform sizes of the nanospheres also suggest a colloidal origin. Colloidal particles will settle if they are larger than the critical size at which the buoyant forces of Brownian movement balance gravitational forces (*27*). For example, colloidal silica particles 150 to 200 nm in diameter are known to settle from suspension (*28*). Specific gravity differences dictate that the critical size of iron hydroxide particles should be slightly smaller than that of silica particles. The observed sizes of the hematite nanospheres in this study are within the range of the estimated critical size (*29*), supporting the proposal that the hematite spheres formed from individual iron hydroxide particles.

The occurrence of hematite nanospheres of colloidal origin, as we suggest, has important implications regarding the condition of deposition and possibly transport of the iron in iron formations. Although it is widely believed that enormous quantities of iron were carried in fluids, whether this iron was transported in the colloidal or ionic states is controversial (*11, 30*). There appears to be broad accord that much iron at Earth's surface in early Precambrian time was in the ferrous state (*5, 8, 31*), a result of the oxygen-poor primitive atmosphere. Howev-

Table 1. Electron-diffraction data of hematite. Reflections correspond to those marked in Fig. 2. Observed *d* values were calculated with the use of the crocidolite in the same specimen as a standard; ss, very strong; s, strong; m, medium; w, weak; ww, very weak. The calculated *d* values are from the data of Blake and Hessevick (*32*): rhombohedral ($R\bar{3}c$), $a = 5.038$ Å; $c = 13.772$ Å; *I*, intensity; obs, observed; calc, calculated.

Reflections	$d(\text{Å})_{obs}$	I_{obs}	$d(\text{Å})_{calc}$	*h*	*k*	*l*
1	3.67	m	3.686	0	1	2
2	2.70	ss	2.703	1	0	4
3	2.50	ss	2.519	1	1	0
4	2.19	m	2.208	1	1	3
5	1.81	m	1.843	0	2	4
6	1.67	s	1.697	1	1	6
7	1.57	ww	1.601	0	1	8
8	1.47	s	1.487	2	1	4
9	1.43	s	1.454	3	0	0
10	1.29	w	1.313	1	0	10
			1.308	1	1	9

er, our TEM data and crystallization mechanisms of hematite nanospheres provide strong evidence for the existence of ferric iron hydroxide particles having a colloidal origin presumably by about 2.5 billion years ago. Such particles raise the question of whether the iron was transported from its source areas in a colloidal state or whether the colloidal particles formed during oxidation in the depositional basins and thus facilitated deposition. Although they are features from a small part of an iron formation, they are widespread in our samples and provide strong direct evidence that colloidal processes were involved in the development of Precambrian iron formations. Other workers should be alert for such potential indicators of the presence and extent of colloidal activity.

REFERENCES AND NOTES

1. H. L. James, *Econ. Geol.* **49**, 235 (1954).
2. H. Lepp and S. S. Goldich, *ibid.* **59**, 1025 (1964); H. L. James and P. K. Sims, *ibid.* **68**, 913 (1973); R. M. Garrels *et al.*, *ibid.* **68**, 1173 (1973); R. C. Morris, *J. Geol. Soc. India* **28**, 227 (1986).
3. A. F. Trendall and R. C. Morris, Eds., *Iron-Formations: Facts and Problems* (Elsevier, Amsterdam, 1983).
4. P. W. U. Appel and G. L. LaBerge, Eds., *Precambrian Iron-Formations* (Theophrastus, Athens, Greece, 1987).
5. P. Cloud, *Econ. Geol.* **68**, 1135 (1973).
6. J. W. Schopf, Ed., *Earth's Earliest Biosphere* (Princeton Univ. Press, Princeton, NJ, 1983).
7. E. S. Barghoorn and S. A. Tyler, *Science* **147**, 563 (1965); P. Cloud, *ibid.* **148**, 27 (1965); *ibid.* **160**, 729 (1968).
8. H. D. Holland, *Econ. Geol.* **68**, 1169 (1973).
9. A. G. Cairns-Smith, *Nature* **276**, 807 (1978); P. Cloud, in (*3*), pp. 401–416; H. D. Holland, *The Chemical Evolution of the Atmosphere and Oceans* (Princeton Univ. Press, Princeton, NJ, 1984).
10. E. S. Moore and J. E. Maynard, *Econ. Geol.* **24**, 272 (1929); *ibid.* **24**, 506 (1929).
11. N. I. Svital'skiy, paper presented at the 17th International Geologic Congress, Moscow (1937); Y. P. Mel'nik, *Precambrian Banded Iron-Formations* (Elsevier, Amsterdam, 1982).
12. C. Klein, Jr., and R. P. Fink, *Econ. Geol.* **71**, 453 (1976).
13. J. H. Oehler, *Geol. Soc. Am. Bull.* **87**, 1143 (1976).
14. D. E. Ayres, *Econ. Geol.* **67**, 1214 (1972).
15. G. A. Gross, *Sed. Geol.* **7**, 241 (1972).
16. G. L. LaBerge, E. I. Robbins, T.-M. Han, in (*4*), pp. 69–96; *Geol. Soc. Am. Bull.* **78**, 331 (1967); P. Cloud and G. R. Licari, *Proc. Natl. Acad. Sci.* **61**, 779 (1968); G. L. LaBerge, *Econ. Geol.* **68**, 1098 (1973); M. S. Lougheed and J. J. Mancuso, *ibid.*, p. 202; J. J. Mancuso, M. S. Lougheed, T. Wygant, *Am. J. Sci.* **271**, 181 (1971); M. S. Lougheed, *Geol. Soc. Am. Bull.* **94**, 325 (1983).
17. P. J. Heaney and D. R. Veblen, in *Geol. Soc. Am. Abstr. Progr.* **24** (1989).

17a. C. Klein, personal communication.

18. W. E. Ewers and R. C. Morris, *Report No. FP23* (CSIRO, Institute of Earth Resources, Division of Mineralogy, Australia, 1980); C. Klein, Jr., and M. J. Gole, *Am. Mineral.* **66**, 507 (1981).
19. Ion-milled specimens were prepared from petrographic thin sections that were cut perpendicular to the bedding direction as seen in drill-core specimens. The microscope we used (JEOL JEM-4000EX) has a top-entry double-tilting sample holder (±15° tilt), a structure resolution limit of 0.17 nm, and a spherical aberration coefficient (C_s) of 1.0 mm. A 40-μm objective aperture and a 150-μm condenser aperture were used for high-resolution TEM imaging. Analytical electron microscopy was performed with a Philips 400T 120-kV transmission electron microscope equipped with a Tracor Northern TN-2000 multichannel analyzer.
20. R. A. Eggleton, *Clays Clay Minerals* **35**, 29 (1987).
21. Eggleton (*20*) described void nucleation as "beginning at a point in the gel where contraction of the surrounding shell away from that point by partial ordering breaks a minimum of bonds between network-forming elements."
22. B. M. French, *Econ. Geol.* **68**, 1063 (1973); E. Dimroth and J. J. Chauvel, *Geol. Soc. Am. Bull.* **84**, 111 (1973).
23. R. J. Floran and J. J. Papike, *J. Petrol.* **19**, 215 (1978).
24. A. A. van der Giessen, *J. Inorg. Nucl. Chem.* **28**, 2155 (1966); T. G. Spiro *et al.*, *J. Am. Chem. Soc.* **88**, 2721 (1966); R. J. Atkinson *et al.*, *J. Inorg. Nucl. Chem.* **30**, 2371 (1968).
25. H. C. Chang, T. W. Healy, E. Matijevic, *J. Colloid Interface Sci.* **92**, 469 (1983); N. Kallay and E. Matijevic, *ibid.* **83**, 289 (1981).
26. R. A. Eggleton *et al.*, *Clay Minerals* **18**, 21 (1983); R. A. Eggleton and J. Keller, *N. Jb. Mineral. Mh. Jg.* **1982**, 321 (1982).
27. E. F. Burton, in *Colloid Chemistry*, J. Alexander, Ed. (The Chemical Catalog Company, New York, 1926), pp. 165–173.
28. R. K. Iler, *The Colloid Chemistry of Silica and Silicates* (Cornell Univ. Press, Ithaca, NY, 1955).
29. The radii of iron hydroxide particles having the same settling velocity (v) as silica particles of 150 to 200 nm are calculated to be 93 to 124 nm from Stokes' law, $v = 2r^2(d_1\text{-}d_2)g/9\eta$. The radius, r, of a particle is proportional to $1/\sqrt{d_1\text{-}d_2}$, where d_1 and d are the specific gravities (G) of the particle and the liquid (water, $G = 1$), respectively and η is the viscosity of the liquid. However, iron hydroxides will have more Brownian movement than silica particles because of their smaller radii, and therefore the critical radius of iron hydroxide particles would be slightly larger than 93 to 124 nm. Specific gravities of silica and iron hydroxide particles are estimated to be 2.4 and 4.7, respectively, on the assumption that they are made of 87.5% quartz ($G = 2.65$) and 12.5% water.
30. B. V. Kaukin, *Akad. Nauk Ukrain. SSR, Inst. Geol. Nauk, Kiev*, **47** (1969); H. P. Eugster and I. Chou, *Econ. Geol.* **68**, 1144 (1973).
31. W. E. Ewers, in (*3*), pp. 491–512; P. S. Braterman and A. G. Cairns-Smith, in (*4*), pp. 215–245.
32. R. L. Blake and R. E. Hessevick, *Am. Mineral.* **51**, 123 (1966).

33. We thank R. C. Morris for providing samples and data, C. M. Lesher and S. Guggenheim for helping us acquire the samples, R. A. Eggleton for valuable suggestions, T. M. Han, H. D. Holland, C. Klein, and G. L. LaBerge for suggestions and reprints, and D. Burt and P. Knauth for helpful reviews. Electron microscopy was performed at the Facility for HREM at Arizona State University (ASU), which is supported by the National Science Foundation (NSF) and ASU. This study was supported by NSF grant EAR-870529.

4 June 1990; accepted 9 July 1990

Different Tumor-Derived p53 Mutants Exhibit Distinct Biological Activities

ORNA HALEVY, DAN MICHALOVITZ, MOSHE OREN*

In its wild-type form, the protein p53 can interfere with neoplastic processes. Tumor-derived cells often express mutant p53. Full-length mutant forms of p53 isolated so far from transformed mouse cells exhibit three common properties in vitro: loss of transformation-suppressing activity, gain of pronounced transforming potential, and ability to bind the heat shock protein cognate hsc70. A tumor-derived mouse p53 variant is now described, whose site of mutation corresponds to a hot spot for p53 in human tumors. While absolutely nonsuppressing, it is only weakly transforming and exhibits no detectable hsc70 binding. The data suggest that the ability of a p53 mutant to bind endogenous p53 is not the sole determinant of its oncogenic potential. The data also support the existence of gain-of-function p53 mutants.

THE CELLULAR PHOSPHOPROTEIN p53 is expressed aberrantly in a variety of neoplastic cells (*1*). Plasmids encoding various mutant forms of p53 possess a distinct oncogenic activity both in vitro (*2–6*) and in vivo (*7*), although wild-type (wt) p53 plasmids actually abolish oncogene-mediated focus formation (*8, 9*). Thus, p53 mutants may facilitate cell immortalization and transformation by interfering with a normal function of wt p53 (*5, 8–11*). Indeed, studies involving mouse (*12*) and human (*13–16*) tumors suggest that wt p53 may possess a tumor-suppressor activity, whose elimination may cause the development of many types of neoplasia.

Most transforming variants of p53 studied exhibit a specific interaction with the major heat shock protein cognate, hsc70 (*17*), which may be important in endowing these variants with oncogenic properties (*4, 6*). There are, however, at least two deletion mutants of p53 that can immortalize primary rodent cells in the absence of any detectable complex with hsc70 (*2, 5*).

The formation of a complex between p53 and other proteins, such as the SV40 large T antigen, the adenovirus type 5 58-kD E1b protein, and hsc70, is correlated with an increased intracellular stability of p53 (*4, 18, 19*). Nevertheless, such interactions are not a prerequisite for p53 stabilization (*2, 11, 18, 20, 21*), and the common denominator in all these cases may, in fact, be the inability of mutant p53 molecules to perform their normal function efficiently.

Department of Chemical Immunology, The Weizmann Institute of Science, Rehovot 76100, Israel.

*To whom correspondence should be addressed.